Detection of Weakly-Coupled Scalar Bosons at Thomas Jefferson National Accelerator Facility

A thesis submitted in partial fulfillment of the requirement
for the degree of Bachelor of Science with Honors in
Physics from the College of William and Mary in Virginia,

by Ruth S. Van de Water

Accepted for _____
(Honors, High Honors, or Highest Honors)

_____
Advisor: Christopher D. Carone, Physics, W&M

_____
Marc Sher, Physics, W&M

_____
Gina Hoatson, Physics, W&M

_____
Richard L. Kiefer, Chemistry, W&M

Williamsburg, Virginia
May 2000

Acknowledgements

I would first like to thank my advisor, Chris Carone. He patiently taught me Quantum Field Theory even though this was often a frustrating, seemingly impossible task. He was amused when I was enthusiastic to the point of hyperactivity, and he was encouraging when I occasionally panicked and felt that I was too stupid to ever be a particle theorist. Most of all, he was able to answer almost all of my neverending stream of questions. Throughout this year, Chris taught me a lot about physics, about research, and about my own capabilities as a physicist. I only hope that I can one day do for my students what he has done for me.

Next, I would like to thank my other committee members — Marc Sher, Dick Kiefer, and Gina Hoatson. While I did not particularly enjoy answering questions at my defense or making revisions to my thesis, they were both important parts of the process and good learning experiences. My final thesis document is better because of them.

Finally, I need to thank Paul King. He gave significant amounts of his time to help me with LaTeX — from formatting to making Feynman diagrams. He proof-read my thesis and corrected both grammatical and physics mistakes. Most importantly, he was there for me when I was incredibly stressed and wanting to just give up. Without him, both my thesis and my life would have fallen apart.

Contents

List of Figures

List of Tables

1 Introduction

1.1 Motivations

In the search for new, exotic particles, physicists are demanding colliders with increasingly high energies. Their goal is to probe the high energy frontier and produce new particles with a rest mass greater then the center of mass energy of existing colliders. Particle physicists tend to pay less attention to the possibility of undiscovered light particles because of a theoretical prejudice: "If it's light enough to be produced, we would have seen it already." However, there is also another frontier in particle physics — light particles that interact weakly. For example, neutrinos exist but are difficult to detect directly. They can actually pass through light years of lead. Other possible light particles are axions, which are pseudoscalars that arise in some extensions of the standard model, and millicharged particles, which have tiny couplings to photons because of their small, fractional electric charge. Examples of theories or extensions of the standard model which motivate the existence of millicharged scalar or pseudoscalar particles can be found in Refs. [1–4]. Detection of such weakly coupled particles at colliders requires a high luminosity incident beam in order to achieve significant event rates. The photon beam at JLab has a high luminosity of approximately $10^{34}\text{cm}^{-2}\text{s}^{-1}$. Our goal is to determine if weakly interacting particles coupling only to photons could be observed at JLab while remaining undetected at other colliders.

1.2 Toy Model

Because JLab has such an intense photon beam, it is particularly sensitive to scattering processes involving photons. To take advantage of this, we choose to design a model particle that interacts with photons. Both scalar and pseudoscalar particles can couple to two photons, but we will consider only the scalar case. Our model particle, which we call a phi particle, ϕ, is a scalar, spin zero boson with zero charge

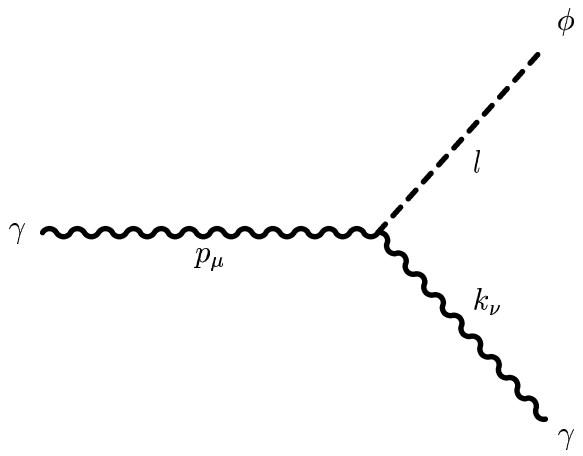

Figure 1: Phi-Photon Vertex with particle momenta p, k, and l

that weakly couples to two photons with a small, dimensionful coupling constant λ. The simplest gauge invariant Lagrangian term that describes this interaction contains a scalar field, two photon fields, and a dimensionful coupling constant. The interaction term in our model Lagrangian is therefore:

$$\mathcal{L} = \lambda \Phi F^{\mu\nu} F_{\mu\nu} \tag{1}$$

where Φ is the field of the phi particle and $F_{\mu\nu}$ is the photon field strength tensor $(\partial_\mu A_\nu - \partial_\nu A_\mu)$. Consequently, our particle only interacts with other particles through the vertex shown in Fig. 1. Using the form of the interaction Lagrangian, the momentum-space representation of this vertex to be used in conjunction with other Feynman rules is:

$$vertex = -4i\lambda[p \cdot k g^{\mu\nu} - k^\mu p^\nu] \tag{2}$$

Here $g^{\mu\nu}$ is the metric tensor.

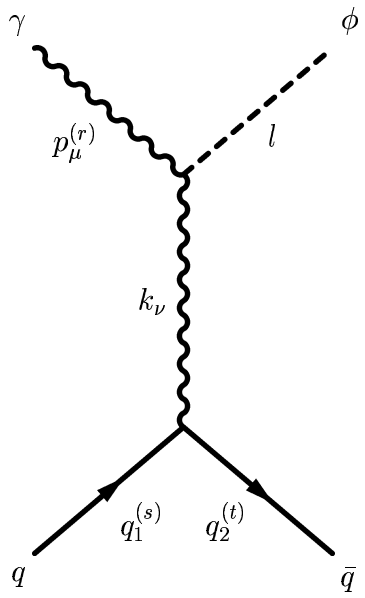

Figure 2: Phi Production at JLab with particle momenta p, k, l, q_1, and q_2

2 Phi Production at JLab

2.1 Production Mechanism

A common type of experiment at Jlab is photoproduction using a photon beam incident upon a proton target. Therefore, the phi particle can be produced by the scattering process in Fig. 2. This process involves the photon interacting with a single quark in the proton, rather than with the entire proton. After the phi particle is created it will again decay to two photons, producing a potentially identifiable peak in the diphoton invariant mass spectrum that corresponds to the particle's mass. This is analogous to the common decay $\pi^0 \rightarrow 2\gamma$, but with a different invariant mass and mean lifetime. For coupling strengths in which our particle is extremely long-lived, identification of these peaks will provide a means of separating signal from background, as we will discuss later.

To determine the phi particle's detectability, we must first calculate its cross section. This represents the effective area per target scattering center that will interact with the incident photon beam. It depends on the mass of the particles, the coupling constant, and the beam energy. The cross section is important because the event rate

is the cross section times the beam luminosity. Therefore, it allows us to predict the phi particle production rate at JLab in terms of various parameters, such as the phi mass, coupling constant, and beam energy.

2.2 Scattering Amplitude

Cross sections are calculated using Feynman rules which give mathematical meaning to each line and vertex in scattering diagrams. Using the Feynman rules for scalars and Quantum Electrodynamics (QED) as well as Eq. (2), the expression for the scattering amplitude for the process shown in Fig. 2 is:

$$iM = \epsilon_{\mu}^{(r)}(p)(-4i\lambda)(p \cdot k g^{\mu\nu} - k^{\mu}p^{\nu})\frac{-ig_{\nu\alpha}}{k^2}\bar{u}^{(t)}(q_2)(iQe\gamma^{\alpha})u^{(s)}(q_1) \tag{3}$$

Here the $\epsilon_{\mu}^{(r)}(p)$ is the polarization vector of the incoming photon; r ranges from one to two for the two polarization states. The next term is the phi particle-photon vertex, and then the photon propagator. The u and $\bar{u}$ are the momentum space spinor wavefunctions for the incoming and outgoing quarks, and they surround the quark-photon vertex. Q is the quark charge in units of the positron's charge. A detailed explanation of Feynman rules and how to use them can be found in Ref. [5].

When determining the squared amplitude, it is important to average over initial spin and polarization states and sum over final spin and polarization states. This is because we assume unpolarized incident states, and it does not matter what the spin and polarization of the final states are if we are simply counting phi particles. The squared amplitude is therefore:

$$\begin{aligned}\frac{1}{4}\sum_{spins}|M|^2 &= \frac{-32Q^2e^2\lambda^2}{k^4}[(p \cdot k)^2 m_q^2 - (p \cdot k)(k \cdot q_1)(p \cdot q_2) \\ &\quad - (p \cdot k)(p \cdot q_1)(k \cdot q_2) + k^2(p \cdot q_1)(p \cdot q_2)]\end{aligned} \tag{4}$$

2.3 Kinematics

Because the squared amplitude depends only on Lorentz invariant quantities, it can be evaluated in any reference frame. We choose the center of momentum (COM)

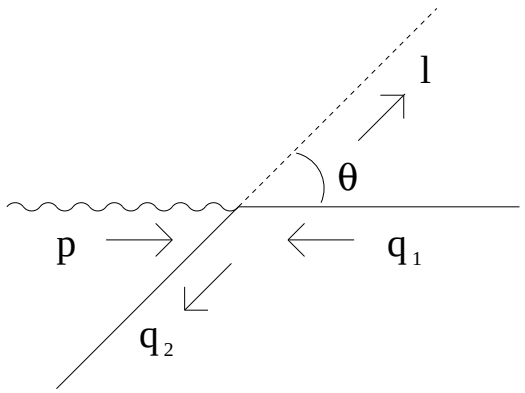

Figure 3: Center Of Momentum Frame Kinematics

frame to simplify calculations. The differential cross section can be re-expressed in terms of lab-frame variables later. It does not matter that various colliders have different beam energies because the cross section is invariant under Lorentz boosts along the beam direction. This is because the cross section is an area in the x-y plane perpendicular to the beam direction, but a boost along the beam direction only causes a Lorentz contraction in the z direction. The kinematics in the COM frame is shown in Fig. 3 and the particle momenta (see Fig. 2) evaluated in the COM frame are:

$$p = (E,\ 0,\ 0,\ E) \tag{5}$$

$$q_1 = (\sqrt{E^2 + m_q^2},\ 0,\ 0,\ -E) \tag{6}$$

$$l = (\sqrt{l_\phi^2 + m_\phi^2},\ 0,\ l_\phi \sin\theta,\ l_\phi \cos\theta) \tag{7}$$

$$q_2 = (\sqrt{l_\phi^2 + m_q^2},\ 0,\ -l_\phi \sin\theta,\ -l_\phi \cos\theta) \tag{8}$$

$$k = (\sqrt{l_\phi^2 + m_\phi^2} - E,\ 0,\ l_\phi \sin\theta,\ l_\phi \cos\theta - E) \tag{9}$$

Here m_q is the quark mass, m_ϕ is the phi mass, and θ is angle between $\vec{l}$ and the beam direction in the COM frame. k is the momentum transfer shown in Fig. 2. Note that the three-momentum l_ϕ is not another variable parameter, but is determined by conservation of energy.

At JLab, each photon scatters off a quark that is in a proton. We therefore introduce a new variable, Bjorken x, which is the fraction of the proton's momentum that the particular quark carries in the infinite momentum frame. This may seem like a strange and unrealistic frame to deal with, but because the transverse momentum of the proton goes to zero in this frame, it allows us to make some useful approximations. The mass of the quark is then related to the mass of the proton by $m_q \sim x m_p$ and the COM energy of the quark-photon interaction, $\sqrt{\hat{s}} = E + \sqrt{E^2 + m_q^2}$, is related to the COM energy of the proton-photon interaction, $\sqrt{s}$, by $\hat{s} \sim xs$. The four-vectors in Fig. 2 can therefore be re-expressed in terms of s, m_p, m_ϕ , and x.

2.4 Parton versus Proton

In general, the expression for the differential cross section for two particles A and B scattering to two particles 1 and 2 is:

$$\frac{d\sigma}{d\Omega} = \frac{1}{2E_A 2E_B |v_A - v_B|} \frac{|\vec{p_1}|}{(2\pi)^2 4E_{CM}} |M(p_A, p_B \to p_1, p_2)|^2 \tag{10}$$

Substituting in for all the relevant quantities and integrating over the azimuthal angle yields the differential cross section, with respect to $\cos\theta$, for scattering off an individual quark in a proton. For example, the differential cross section for scattering off an up quark is shown in Fig. 4 with the parameters $m_\phi = 1$ GeV, $\lambda = 10^{-6}$ GeV^{-1}, and $E_{CM} = 4$ GeV. We observe that $\frac{d\sigma}{d\cos\theta}$ grows rapidly as $\cos\theta$ approaches 1. This is because in the $m_q = 0$ limit, k$^2 \to 0$ as $\cos\theta \to 1$. Therefore the photon propagator goes on-shell and the amplitude blows up. In our calculations, m_q is small but finite, so the differential cross section simply gets big, but does not go to infinity, in this region. However, k^2 does not go to zero and the photon propagator does not go on-shell in the $m_q = 0$ limit for $\cos\theta = -1$, so the plot is asymmetric.

Quantum Chromodynamics (QCD) forbids the existence of isolated quarks because they are not color neutral. Our target proton actually consists of two ups and a down quark, as well as any number of virtual up, down, and strange quark-

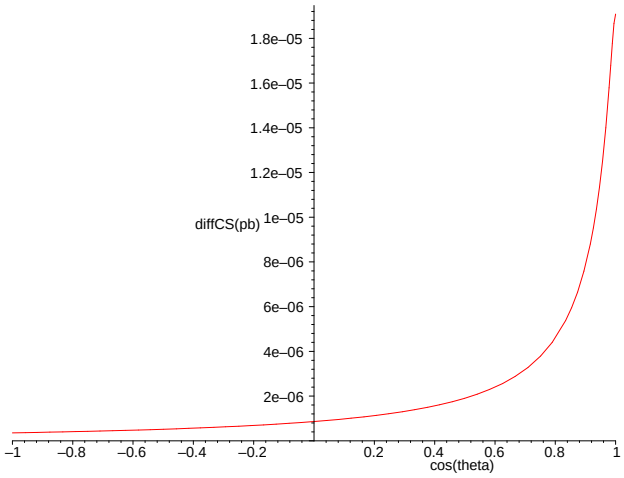

Figure 4: Plot of a Sample Up Quark Differential Cross Section

antiquark pairs. To find the total differential cross section, we must therefore take into account all of these different quarks and their distributions within the proton. This requires knowing the parton distribution functions of the quarks in the proton. These functions weight each quark differential cross section according to the probability of scattering off of that particular type of quark in the proton, with a given momentum fraction x. We use the following numerical approximations for the quark distribution functions in terms of Bjorken x [6]:

$$u_v = 2.188\frac{(1-x)^3}{\sqrt{x}} \tag{11}$$

$$d_v = 1.230750\frac{(1-x)^4}{\sqrt{x}} \tag{12}$$

$$u_{sea} = 0.186\frac{(1-x)^7}{x} \tag{13}$$

$$d_{sea} = 0.186\frac{(1-x)^7}{x} \tag{14}$$

$$s_{sea} = 0.0930\frac{(1-x)^7}{x} \tag{15}$$

Here u_v and d_v are for the up and down valence quarks and u_{sea}, d_{sea}, and s_{sea} are for the up, down, and strange sea quarks. The parton distributions are normalized

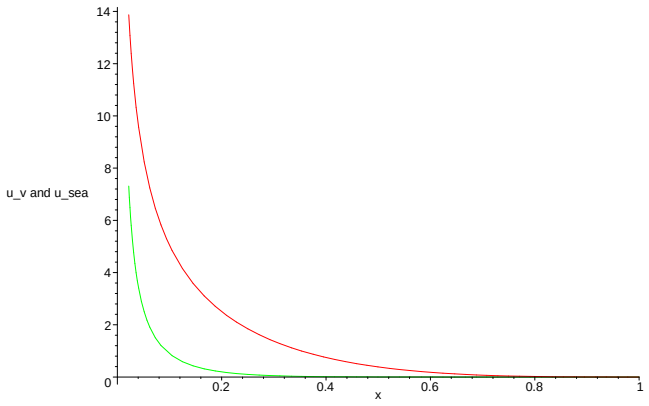

Figure 5: Plot of u_v (upper line) and u_{sea} (lower line) v. Bjorken x

such that:

$$\sum_i \int_0^1 x(\text{parton distribution function})_i dx = 1 \tag{16}$$

An example plot of u_v and u_{sea} is shown in Fig. 5. Notice that the sea quarks only contribute significantly at low fractional momenta.

2.5 Total Cross Section

To get the total cross section, we must multiply the quark differential cross sections by the appropriate parton distribution functions and integrate over $\cos\theta$ and all possible momentum fractions. The lower bound on x is determined by the fact that for fixed s, $\sqrt{\hat{s}}$ must be greater than or equal to $m_\phi + m_q$ in order to create the two final state particles. The upper bound on x is 1, while $\cos\theta$ ranges from -1 to 1. The total cross section is therefore:

$$\sigma = \int\int \frac{d\hat{\sigma_u}}{d(\cos\theta)}(u_v + 2u_{sea}) + \frac{d\hat{\sigma_d}}{d(\cos\theta)}(d_v + 2d_{sea} + 2s_{sea})\; dx\; d(\cos\theta) \tag{17}$$

where $\frac{d\hat{\sigma_u}}{d(\cos\theta)}$ is the up quark differential cross section and $\frac{d\hat{\sigma_d}}{d(\cos\theta)}$ is the down quark differential cross section.

Because the final expression for the total cross section is extremely large and complicated, I wrote Maple code in December to numerically do the x integration and then plot the total differential cross section versus $\cos\theta$ for specific values of m_ϕ

$\sqrt{s}$ (GeV)	λ (10^{-6}GeV^{-1})	m_ϕ (GeV)	Total Cross Section (10^{-6}pb)	color
2.25	1	1	1.75	red
3.25	1	1	13.76	green
4.0	1	1	41.24	yellow
4.0	1	2	2.32	blue

Table 1: Total Cross Sections Generated Numerically Using C++ Code

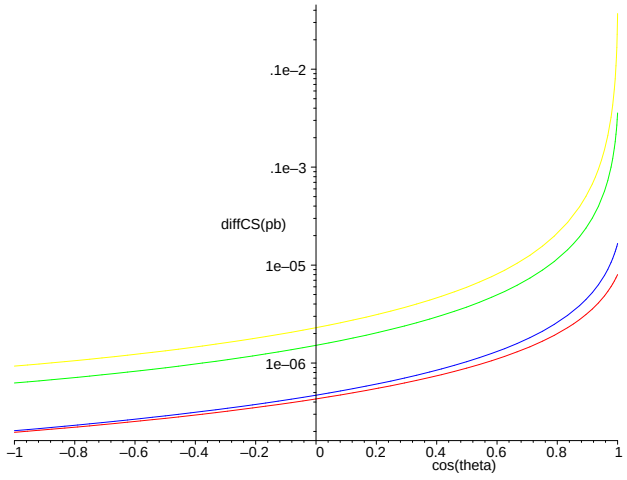

Figure 6: Differential Cross Sections v. $\cos\theta$ for values of $\sqrt{s}$, λ, and m_ϕ assumed in Table 1

and λ. Some examples of these plots are shown in Fig. 6. The area under these curves give an initial visual estimate for the total cross section. However, Maple is not particularly effective at numerical work, so C++ code was written to perform the numerical integrations more efficiently.

Total cross section results for the same values of m_ϕ, λ, and $E_{CM} = \sqrt{s}$ as chosen in Fig. 6 are shown in Table 1. These numbers were generated by a modified version of the code shown in Appendix F. Note that the strong energy dependence of these results can be understood qualitatively. Figure 7 shows up quark differential cross

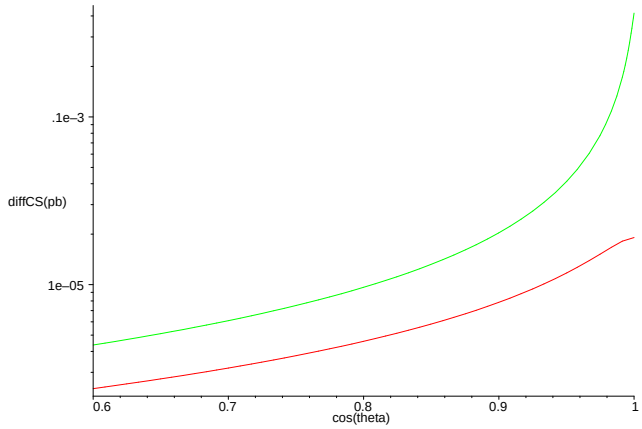

Figure 7: Up Quark Differential Cross Sections for $\sqrt{\hat{s}} = 2.25$ GeV (red) and $\sqrt{\hat{s}} = 3.25$ GeV (green)

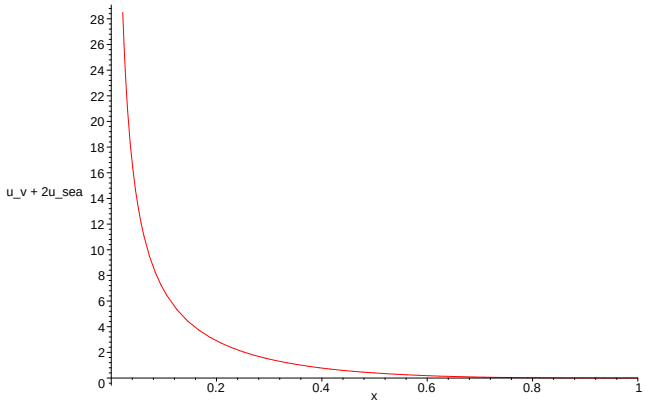

Figure 8: $(u_v + 2u_{sea})$ v. Bjorken x

sections for $\sqrt{s} = 2.25$ GeV and $\sqrt{s} = 3.25$ GeV. At $\cos\theta = 0$, the top plot is only a factor of 1.6 larger than the bottom. However, by the time $\cos\theta$ reaches 1 the top plot is larger than the bottom by a factor of 21. From Figure 7 we estimate the area under the top curve to be roughly 3 times that under the bottom curve. However, this only partially accounts for the large difference between the cross sections in rows 1 and 2 of Table 1. Figure 8 shows a plot of $u_v + 2u_{sea}$ versus the fractional momentum x. Changing the COM energy also changes the lower limit of x integration. From this plot it is easy to see that a small change in the lower limit of x integration can cause a large change in the parton distribution function, and therefore the total cross section. For $\sqrt{s} = 2.25$ GeV, the lower limit of x integration is .24, while for $\sqrt{s} =$

3.25 GeV it is .12. This increases $u_v + 2u_{sea}$ by a factor of 2.6. Multiplying the cross section in row 1 by 3×2.6 gives a cross section of 13.65 pb, which is quite close to row 2's value of 13.76, as it should be.

As another cross-check, we make an order-of magnitude estimate of the cross section based on the expression for the squared amplitude in Eq. (4). We observe that the cross section is proportional to $32e^2\lambda^2$. Assuming that the energy and momentum terms are of order one, we multiply these factors by an additional $\frac{1}{16\pi^2}$ from integrating over the two-body Lorentz-invariant phase space. Therefore the cross section should be on the order of $\frac{32\alpha\lambda^2}{4\pi}$, or 10^{-14} GeV^{-1}. This corresponds to 10^{-6}pb, which is the same order-of-magnitude as the cross sections in Table 1. We are therefore confident that our C++ code generates cross sections that display the proper E_{CM}-dependent behavior and are of the correct order-of-magnitude.

3 Constraints on Parameter Space

3.1 Overview

Throughout the calculations described in Section 2, both λ and m_ϕ remain undetermined constants. Consequently, we are free to vary these parameters in order to change the phi production rate at JLab. However, certain regions in λ–m_ϕ parameter space can already be excluded by using data from collider and hadronic decay experiments. We can also isolate interesting regions based on knowledge of how the phi particle decays. In these sections we will calculate these constraints and, by plotting them simultaneously, we will visually determine the allowed regions of the λ–m_ϕ plane. We will then calculate phi production rates at JLab for values of λ–m_ϕ in this parameter space and see whether or not they are potentially large enough for phi to be detected.

3.2 e^+e^- to γ Plus Missing Energy

The first constraint comes from data taken by the L3 Collaboration at LEP, where they are determining the number of light neutrino species [7]. They produce neutrinos via the process $e^+e^- \rightarrow \nu\bar{\nu}\gamma$. The lowest order Feynman diagrams that contribute to this process are shown in Fig. 9. Neutrinos have incredibly small cross sections and long lifetimes so they are not detected directly. Therefore, experimenters look for electron-positron collisions that produce a single photon plus missing energy. This missing energy corresponds to the undetected neutrinos.

Another process that can occur at LEP and produce a single photon plus missing energy is production of the phi particle as shown in Fig. 10. Because the phi has zero charge, it will not leave a track in the time expansion chamber (TEC) which looks for charged particles. Also, because it only couples very weakly to photons, it will not deposit any energy in the electromagnetic calorimeter. Consequently, the phi particle will remain undetected and its production will leave an identical signal

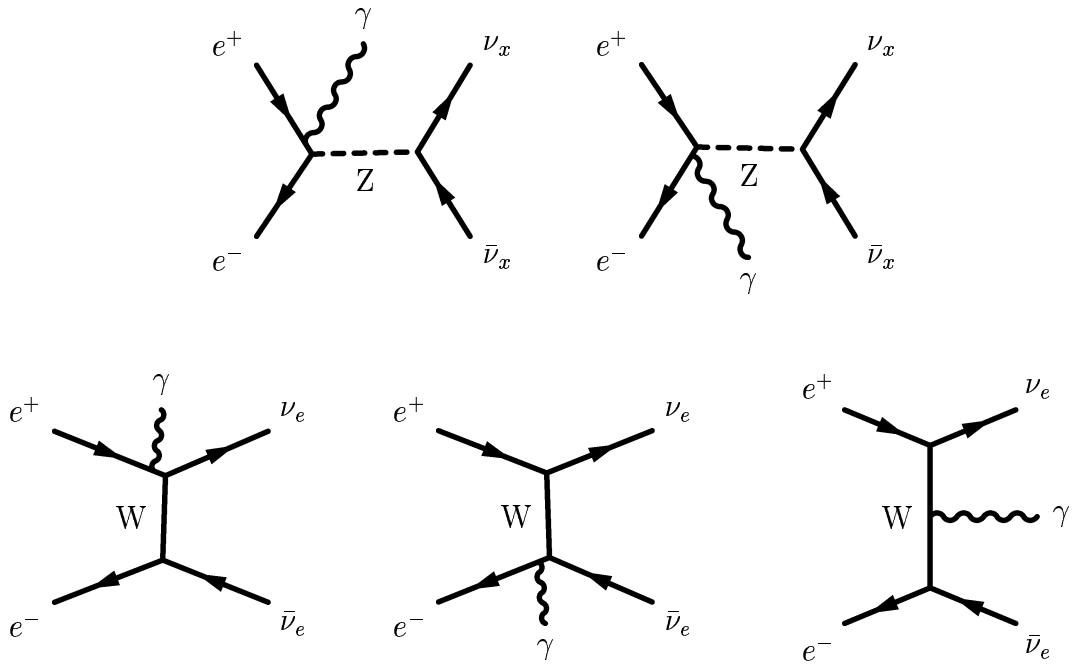

Figure 9: Lowest Order Contributions to Neutrino Production at LEP

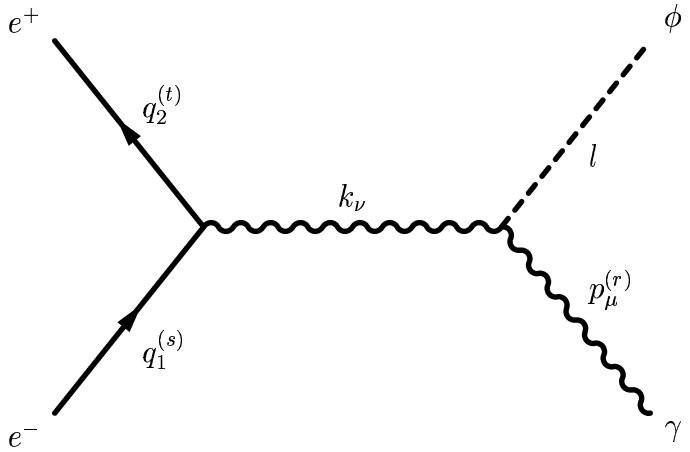

Figure 10: Phi Production at LEP with particle momenta q_1, q_2, k, l, and p

to that of neutrino production. However, we know that the cross section for this method of phi production is small and bounded by the error bars on the cross section measurements for neutrino production. This is because the cross sections measured by the L3 collaboration agree within error measurements to predictions based on the standard model, which we believe correctly describes the physics of how particles interact. If the cross section for phi production were bigger than the error bars and caused experimental disagreement with standard model predictions, we would assume that there was an unknown process creating a single photon plus missing energy. Thus the phi particle would already have been detected. We therefore constrain the cross section for phi production to be smaller than the error bars on the cross section for neutrino production.

The squared amplitude for the scattering in Fig. 10 is:

$$|M|^2 = \frac{32e^2\lambda^2}{k^4}[m_e^2(p\cdot k)^2+(p\cdot k)(p\cdot q_1)(k\cdot q_2)+(p\cdot k)(p\cdot q_2)(k\cdot q_1)-k^2(p\cdot q_1)(p\cdot q_2)] \quad (18)$$

The cross section (in picobarns) in terms of the COM energy (in GeV) for a polar angle between 45^0 and 135^0, which is the same range examined by L3, is:

$$\sigma = \frac{\alpha\lambda^2}{2E_{CM}^7}\frac{(E_{CM}^2-m_\phi^2)^3}{\sqrt{\frac{E_{CM}^2}{4}-m_e^2}}[\frac{2m_e^2}{\sqrt{2}}+\frac{E_{CM}^2}{2\sqrt{2}}+\frac{1}{3\sqrt{2}}(\frac{E_{CM}^2}{4}-m_e^2)] \quad (19)$$

Adriani *et al.*[7] give the experimentally determined cross sections for an electron-positron collision producing a single photon plus missing energy at various center of mass energies. We substitute each E_{CM} into Eq. (19) to determine the phi production cross section in terms of λ and m_ϕ. We then constrain our calculated cross section to be less then the experimental error bars on their cross section. Specifically, for E_{CM} = 91.25 GeV and $\sigma(e^+e^- \to \nu\bar{\nu}\gamma) = 37$ pb, the phi production cross section must be less than 4 pb, which yields the plot for λ v. m_ϕ shown in Fig. 11. The allowed region in parameter space lies below this line. Each value of E_{CM} gives a slightly different plot because of the differing error bars, but the one shown above gives the tightest bound.

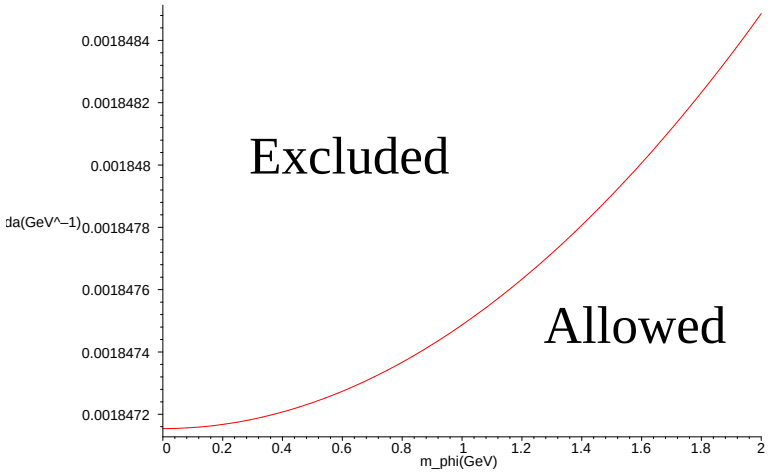

Figure 11: Constraint Based on e^+e^- Scattering at LEP

3.3 $\Upsilon(1S)$ to γ Plus Unseen Particle

The second constraint on λ v. m_ϕ comes from data taken by the CLEO Collaboration at the Cornell Electron Storage Ring(CESR) [8]. They determine the branching ratio of the decay $\Upsilon(1S) \to \gamma X$ to be less than 10^{-5}. $\Upsilon(1S)$ is a heavy quark bound state consisting of a $b\bar{b}$ pair and X is any particle that experimenters do not see, either because it is outside the detector's acceptance or because it is noninteracting. In any two body decay, the momenta of the decay products are entirely determined by the particle masses. Experimenters such as those at CLEO therefore search for monochromatic (single energy) photons. One decay that produces this type of signal is shown in Fig. 12. This decay is allowed under charge and parity conjugation, as is shown in Ref. [9]. Because ϕ is not charged and has only an extremely weak coupling to photons, it will not leave a track in the drift chambers or deposit energy in the electromagnetic calorimeter. It will simply pass through the detectors unobserved. The experimentally determined upper limit on BF$(\Upsilon(1S) \to \gamma X)$ is therefore also an upper limit on BF$(\Upsilon(1S) \to \gamma\phi)$, and can be used to get another bound on λ v. m_ϕ.

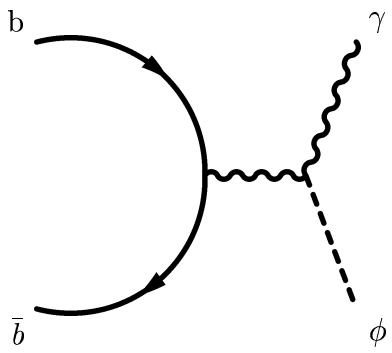

Figure 12: $\Upsilon(1S)$ Decay to Photon Plus ϕ

The branching fraction of $\Upsilon(1S) \to \gamma\phi$ is defined by:

$$BF(\Upsilon \to \gamma\phi) = \frac{\Gamma(\Upsilon \to \gamma\phi)}{\Gamma_{tot}} \tag{20}$$

Although this does not seem particularly useful, because in order to calculate Γ_{tot} we need to calculate the decay width for all possible decays of $\Upsilon(1S)$, we can get around this problem by relating Γ_{tot} to a branching ratio that has been well determined experimentally, such as that for $\Upsilon(1S) \to \mu^+\mu^-$. We therefore substitute this in for Γ_{tot}:

$$\Gamma_{tot} = \frac{\Gamma(\Upsilon \to \mu^+\mu^-)}{BF(\Upsilon \to \mu^+\mu^-)} \tag{21}$$

Now, after applying the experimental constraint, we have the simple equation:

$$BF(\Upsilon \to \gamma\phi) = \frac{\Gamma(\Upsilon \to \gamma\phi)}{\Gamma(\Upsilon \to \mu^+\mu^-)} BF(\Upsilon \to \mu^+\mu^-) \leq 10^{-5} \tag{22}$$

and all we need to calculate are two decay widths.

However, even this is not trivial because $\Upsilon(1S)$ is a bound state. We cannot simply write down the scattering amplitude for this process using the Feynman rules for QED. Since the Υ(1s) is a vector meson, we will assume an effective photon-Υ interaction of the form $\zeta F^{\gamma}_{\mu\nu} F^{\mu\nu}_{\Upsilon}$, and the size of this interaction, ζ, will cancel in the ratio in Eq. (22). This is the simplest possible gauge-invariant interaction between the photon and a "massive photon." This approach should be sufficient for an order of magnitude estimate of the bounds. The shaded in circle in Fig. 13 represents our

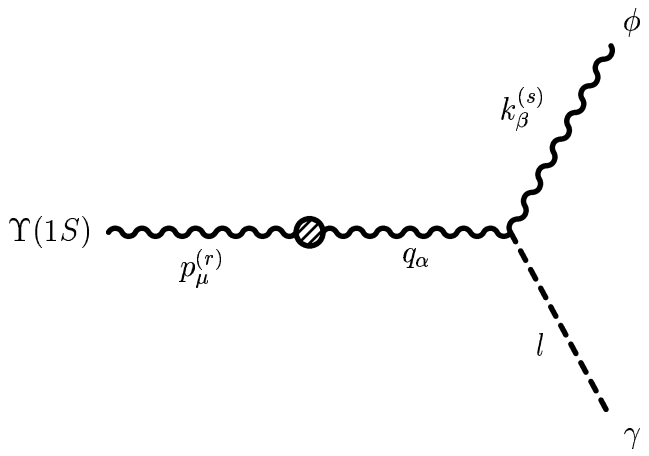

Figure 13: New Feynman Diagram for $\Upsilon(1S) \to \gamma\phi$ with particle momenta p, q, k, and l

new gauge-invariant vertex. The expression for this vertex in momentum space is:

$$new\ vertex = \zeta[p \cdot q g^{\mu\nu} - q^\mu p^\nu] \tag{23}$$

The scattering amplitude for this process is then:

$$iM = \epsilon_\mu^{(r)} \zeta[p \cdot q g^{\mu\nu} - q^\mu p^\nu] \frac{-ig_{\nu\alpha}}{q^2} (-4i\lambda)[q \cdot k g^{\alpha\beta} - k^\alpha q^\beta] \epsilon_\beta^{*(s)} \tag{24}$$

and the squared amplitude after evaluating the kinematics in the rest frame of the Υ is:

$$|M|^2 = 2\lambda^2\zeta^2(m_\Upsilon^2 - m_\phi^2) \tag{25}$$

In general, the decay width for a particle A decaying to two final state particles, each with three-momentum $\vec{p}$ in the COM frame is:

$$d\Gamma = \frac{1}{m_A} \int \frac{d\Omega_{CM}}{32\pi^2} \frac{|\vec{p_1}|}{E_{CM}} |M(m_A \to p_1, p_2)|^2 \tag{26}$$

Therefore the decay width for this process is:

$$\Gamma(\Upsilon \to \gamma\phi) = \frac{\lambda^2\zeta^2}{8\pi} \frac{(m_\Upsilon^2 - m_\phi^2)^3}{m_\Upsilon^3} \tag{27}$$

Similarly, the new Feynman diagram for $\Upsilon(1S) \to \mu^+\mu^-$ is shown in Fig. 14. The decay width for this process is:

$$\Gamma(\Upsilon \to \mu^+\mu^-) = \frac{e^2\zeta^2}{16\pi} \sqrt{\frac{m_\Upsilon^2}{4} - m_\mu^2} \frac{8m_\mu^2 + m_\Upsilon^2}{m_\Upsilon^2} \tag{28}$$

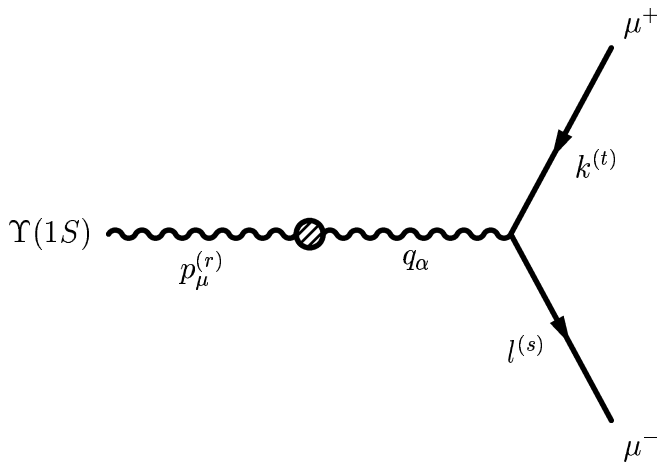

Figure 14: New Feynman Diagram for $\Upsilon(1S) \to \mu^+\mu^-$ with particle momenta p, q, k, and l

Plugging both decay widths as well as the experimentally measured branching fraction [10] for $\Upsilon(1S) \to \mu^+\mu^-$ into Eq. (22) yields:

$$\frac{(.0248)\lambda^2}{\pi\alpha}\frac{(m_\Upsilon^2 - m_\phi^2)^3}{2m_\mu^2 m_\Upsilon + m_\Upsilon^3}(\frac{m_\Upsilon^2}{4} - m_\mu^2)^{-1/2} \leq 10^{-5} \tag{29}$$

A plot of λ v. m_ϕ is shown in Fig. 15. Our constraint is therefore that ϕ must live below this line in parameter space.

3.4 Phi Decay Distance

The third "constraints" are not actually physical bounds on the phi particle's existence. Rather, we impose certain requirements in order to help distinguish a phi particle signal from background. The first requirement is that ϕ must never decay within existing JLab detectors. Thus we can set up our detector farther away and eliminate many background peaks in the diphoton invariant mass spectrum that are due to decays of shorter-lived particles. Also, our experiment can then be run continuously, independent of and not interfering with the primary experiment at the time. The second requirement is that ϕ must decay within JLab's facilities. This

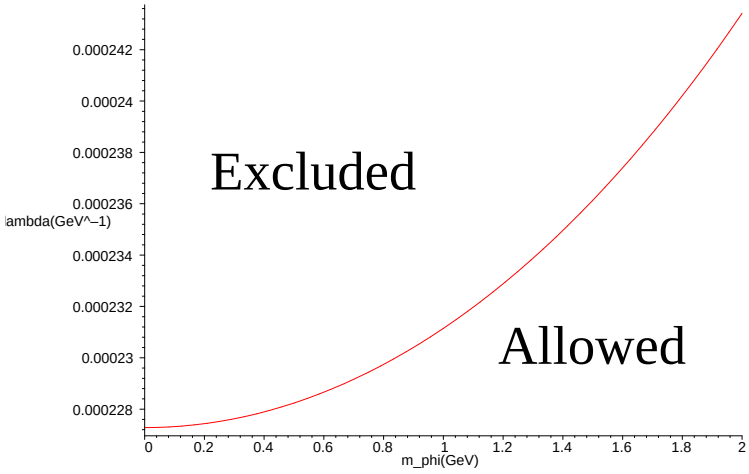

Figure 15: λ v. m_ϕ Constraint Based on $\Upsilon(1S)$ Decay

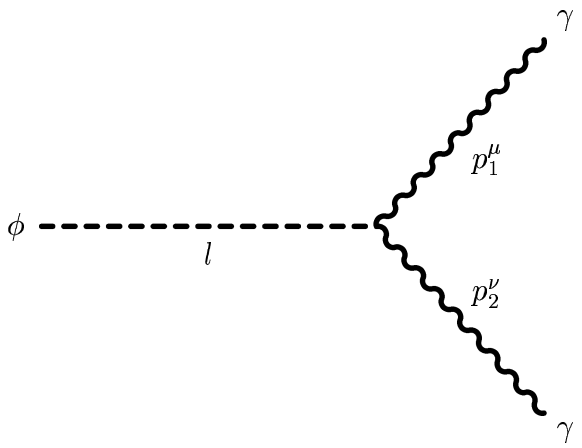

Figure 16: Phi Decay Process with particle momenta l, p_1, and p_2

insures that it decays somewhere that we can actually set up a detector.[1]

The phi particle decays into two photons as shown in Fig. 16. The squared amplitude for this process is:

$$|M|^2 = 32\lambda^2(p_1 \cdot p_2)^2 \tag{30}$$

The general decay width for a particle A decaying to two final state particles, each with three-momentum $\vec{p}$ in the COM frame is shown in Eq. (26). The phi particle's

[1]For much smaller couplings, one could imagine setting up a detector at a distant site. We don't consider this possibility here.

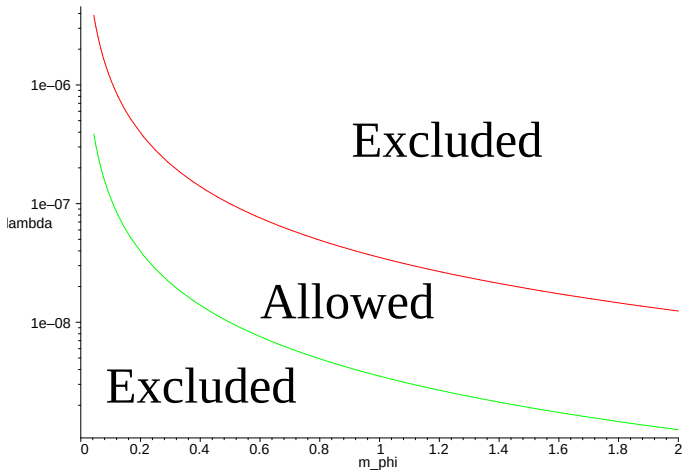

Figure 17: λ v. m_ϕ Constraints Based on Phi's Decay Distance for d = 100m (upper) and d = 1m (lower)

decay width is therefore:

$$\Gamma = \frac{\lambda^2 {m_\phi}^3}{2\pi} \tag{31}$$

The mean lifetime of the phi particle is simply $\frac{\hbar}{\Gamma}$, so the distance that the phi particle travels before it decays is $\frac{c\hbar}{\Gamma}$, or:

$$d = \frac{c\hbar 2\pi}{\lambda^2 {m_\phi}^3} \tag{32}$$

We make the order-of-magnitude estimates that the phi particle must travel at least one meter before it decays, so it is well outside existing detectors, but must decay before it travels 100 meters, so it is within the JLab site where we can set up a detector. Plotting these constraints in λ v. m_ϕ parameter space yields the two curves shown in Fig. 17. The allowed λ–m_ϕ parmeter space lies between the curves. Parameters in this range also satisfy the previous bounds shown in Figure 11 and Figure 15. We therefore only need to consider this area in parameter space.

3.5 Light-by-Light Scattering

We now need to know if these calculations are sufficient or if we could achieve even tighter bounds than those from phi decay by applying more experimental constraints.

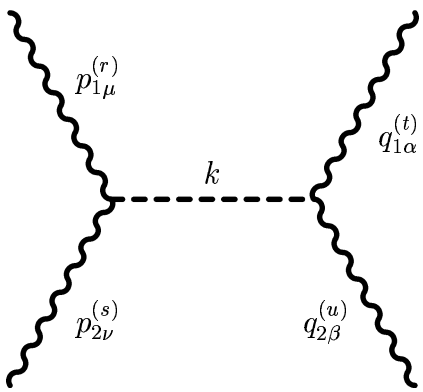

Figure 18: Light-by-Light Scattering via the Phi-Photon Vertex with particle mo menta p_1, p_2, k, q_1, and q_2

The answer is that in this range we are not likely to get any other constraints on the model since the coupling is small compared to 2^{nd} order QED corrections. To illustrate this point, consider light-by-light scattering. Because ϕ couples to two photons, it is a means of scattering light-from-light, as shown in Fig. 18. Ideally, we would like to calculate the cross section for this process and compare it to an experimental value. In this diagram, all of the photon lines are external, so these are real, massless photons. Unfortunately, photon-photon scattering has not yet been done with *real* photons, although it has been done with virtual ones [11]. Therefore we have no experimental cross section for comparison and must turn to theory for assistance.

The QED cross section for real photon-photon scattering involves a number of Feynman diagrams. However, for our purposes an order-of-magnitude estimate is sufficient. The lowest order process that contributes to photon-photon scattering in QED is shown in Fig. 19. The scattering amplitude for this process is approximately:

$$i|M| \sim \frac{e^4}{16\pi^2} \int d^4p \frac{tr(\gamma_\alpha \ldots \gamma_\delta)(\epsilon_\mu \ldots \epsilon_\sigma)}{(\not{p} - m)^4} \tag{33}$$

Here, the e^4 and the four γ-matrices in the numerator come from the QED vertices, the $\not{p} - m$'s in the denominator from the fermion propagators, the four ϵ's from the external photons, and the $\int d^4p$ and $\frac{1}{16\pi^2}$ from the undetermined loop momenta. Because the integral is essentially $\frac{d^4p}{p^4}$ with some $g_{\mu\nu}$'s thrown in, it is of order one.

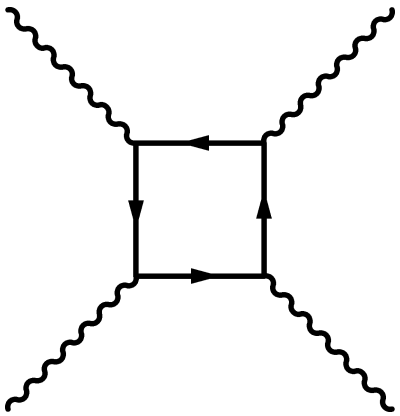

Figure 19: Lowest Order Contribution to Photon-Photon Scattering in QED

This means that:

$$i|M| \sim \frac{e^4}{16\pi^2} \tag{34}$$

and:

$$|M|^2 \sim \frac{e^8}{256\pi^4} = \alpha^4 \tag{35}$$

We will therefore calculate $|M|^2$ for the process in Fig. 18 and compare it to α^4.

The scattering amplitude for Fig. 18 is:

$$i|M| = (-4i\lambda)^2 \epsilon_\mu^{(r)} \epsilon_\nu^{(s)} [p_1 \cdot p_2 g^{\mu\nu} - p_2^\mu p_1^\nu] (\frac{i}{k^2 - m_\phi^2}) [q_1 \cdot q_2 g^{\alpha\beta} - q_2^\alpha q_1^\beta] \epsilon_\alpha^{(t)} \epsilon_\beta^{(u)} \tag{36}$$

and:

$$|M|^2 = 256\lambda^4 \frac{(p_1 \cdot p_2)^2 (q_1 \cdot q_2)^2}{(k^2 - m_\phi^2)^2} \tag{37}$$

Evaluating this in the COM frame:

$$|M|^2 = \frac{16\lambda^4 E_{CM}^8}{(E_{CM}^2 - m_\phi^2)^2} \tag{38}$$

We choose E_{CM} to be 3.35 GeV because it is the maximum COM energy at JLab.[2] We also choose m_ϕ to be 0.1 GeV and λ to be 7.0×10^{-7} GeV^{-1} because they are in the allowed region in parameter space. Using these values, Eq. (38) becomes:

$$|M|^2 = 0.48 \times 10^{-21} \tag{39}$$

[2]The maximum beam energy in the lab frame is 6 GeV, although few photons in the beam actually have this much energy. For a fixed target experiment, $E_{CM} = \sqrt{2 m_T E_B}$, where m_T is the target mass and E_B is the beam energy [12]. Therefore a beam energy of 6 GeV in the lab frame corresponds to an energy of 3.35 GeV in the COM frame.

Comparing this to the QED squared amplitude from Eq. (35):

$$\frac{|M_\phi|^2}{|M_{QED}|^2} = 0.17 \times 10^{-12} \tag{40}$$

This ratio is extremely small. It demonstrates that any 2nd order process involving the phi particle will be negligible compared to the comparable QED process, so we will not get any additional constraints in this manner. We therefore conclude our calculations.

3.6 Event Rates in the Allowed Region

We have just shown four means of getting bounds on the λ-m_ϕ parameter space using theory, experimental data, and practical constraints. Additional constraints can be applied to further reduce the allowed region. Table 2 shows phi production rates at JLab for values of λ and m_ϕ in the allowed region for various COM energies. While a COM energy of 4 GeV is not yet possible at JLab, the beam energy will soon be upgraded to 9 GeV, so it will be attainable in the future [13]. The mass of ϕ is also constrained because the COM energy must be great enough to produce the two final state particles, or $\sqrt{xs} \geq m_\phi + x m_p$. With a beam energy of 2.25 GeV, the mass of the phi particle produced can be at most 1.67 GeV, with $\mathrm{E}_{CM} = 3.25$ GeV $m_\phi \leq$ 2.85 GeV, and with $\mathrm{E}_{CM} = 4.0$ GeV $m_\phi \leq 4.26$ GeV. All of the masses in this table are well within these limits. All numbers converged to within 1% accuracy except for the one which is asterisked, which converged to within 5%.

These results, which were generated by the C++ code in Appendix F, behave as expected with changes in E_{CM}, λ, and m_ϕ.[3] The squared amplitude, and therefore the cross section, is proportional to λ^2. The squared amplitude and individual quark differential cross sections have little dependence on m_ϕ for the values in Table 2 since m_ϕ is significantly smaller than the typical energy scale. However, changing m_ϕ

[3]See Section 2.5 for an explanation of the cross section's dependence on E_{CM}. Because the number of events is simply the σ times the beam luminosity times one year, if the results in Table 1 have the right E_{CM} dependence so do those in Table 2.

E_{beam} (GeV)	E_{CM} (GeV)	λ (10^{-8}GeV^{-1})	m_ϕ (GeV)	Events Per Year
2.23	2.25	70	.1	54.89
2.23	2.25	20	.3	.81
2.23	2.25	8	.5	.04
5.16	3.25	70	.1	140.34
5.16	3.25	20	.3	2.05
8.06	4.0	20	.3	4.14*
8.06	4.0	8	.5	.31
8.06	4.0	4	.8	.03

Table 2: Phi Production Rates at JLab in the Allowed Parameter Space

does change σ by changing the lower limit of x integration. Fig. 20 plots the parton distribution functions versus the momentum fraction, x. At small x values, a minute change in x produces a large change in these functions. Therefore slightly lowering the limit of x integration by decreasing m_ϕ greatly increases the cross section. Rows 1 and 2 in Table 2 illustrate the cross sectional dependence on both λ^2 and m_ϕ. Because σ is proportional to λ^2, cross section one should be a factor of $\frac{70^2}{20^2}$, or $\frac{49}{4}$, larger than cross section two. For row 2, the lower limit of x integration is .009, while for row one it is .0016. This increases $u_v + 2u_{sea}$ by a factor of 4.65 and $d_v + 2d_{sea} + 2s_{sea}$ by a factor of 5.36, but we will call them both 5. Recall that the event rate is proportional to the cross section. Multiplying .81 events, the number of events in row 2, by $\frac{49}{4} \times 5$ gives 49 events, which is quite close to row 1's value of 55 events. We therefore believe that our code works and are confident in the numbers in Table 2.

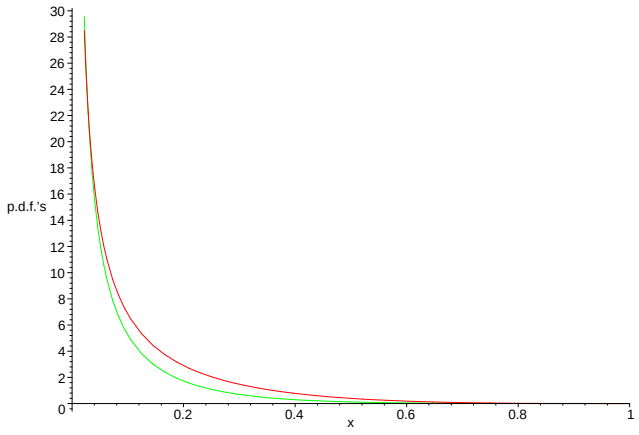

Figure 20: $u_v + 2u_{sea}$ (upper) and $d_v + 2d_{sea} + 2s_{sea}$ (lower) v. Bjorken x

4 Conclusions

These results are promising. If a particle such as ours *does* exist, it is potentially detectable. Our detector will sit outside those of JLab's primary experiment without interfering. Our experiment can therefore run almost continuously, only having to shut down when the beam is turned off. Consequently, even if we have as small a production rate as five phi particles a year, we can run for a few years to achieve a significant number of events.

However, producing enough particles is not the only concern; we must be able to separate signal from background. When a ϕ decays in our detector, it will produce two photons. By knowing their energy and momentum, we can recreate the phi's invariant mass. Thus, we will look for a peak in the diphoton invariant mass spectrum corresponding to the mass of the phi particle. The principal background source of such peaks is pion and heavy meson decay. Fortunately, most heavy mesons that can decay into two photons that are produced in the interaction region are strongly interacting [10] and will therefore decay long before reaching our detector. Pions from cosmic rays pose more of a problem in this respect. However, their decays will appear randomly and not correlate with the recoil of the target proton. Thus by requiring both creation of two photons and recoil of the proton, we might be able to eliminate

background from pion decay. Distinguishing signal from background requires a more detailed analysis.

Finally, we need to address another issue before talking with experimenters. We must examine the realism of our model and perhaps modify it. Such modifications could include adding a different type of interaction term to the Lagrangian or making phi a pseudoscalar particle. We therefore conclude that after applying a variety of constraints, it is possible that a weakly interacting particle coupling only to photons could be detected at JLab while remaining unseen at other colliders such as LEP or CLEO.

A Calculation of $\gamma q \to q\phi$ Differential Cross Section

The Feynman diagram for $\gamma q \to q\phi$ is shown in Fig. 2. The expression for the phi-photon vertex in momentum space is given in Eq. (2). Therefore the scattering amplitude is:

$$iM = \epsilon_{\mu}^{(r)}(p)(-4i\lambda)(p \cdot k g^{\mu\nu} - k^{\mu}p^{\nu})\frac{-ig_{\nu\alpha}}{k^2}\bar{u^{(t)}}(q_2)(iQe\gamma^{\alpha})u^{(s)}(q_1) \tag{41}$$

Contracting up $g_{\nu\alpha}$:

$$iM = \frac{(-4iQe\lambda)}{k^2}\epsilon_{\mu}^{(r)}(p)(p \cdot k g^{\mu\nu} - k^{\mu}p^{\nu})\bar{u^{(t)}}(q_2)(\gamma_{\nu})u^{(s)}(q_1) \tag{42}$$

The squared amplitude is:

$$\begin{aligned} |M|^2 &= \frac{16Q^2e^2\lambda^2}{k^4}\epsilon_{\mu}^{(r)}\epsilon_{\alpha}^{*(r)}(p \cdot k g^{\mu\nu} - k^{\mu}p^{\nu})(p \cdot k g^{\alpha\beta} - k^{\alpha}p^{\beta}) \\ &\quad \bar{u^{(t)}}(q_2)\gamma_{\nu}u^{(s)}(q_1)\bar{u^{(s)}}(q_1)\gamma_{\beta}u^{(t)}(q_2) \end{aligned} \tag{43}$$

Averaging over initial and summing over final spin and polarization states:

$$\begin{aligned} \frac{1}{4}|M|^2 &= \frac{4Q^2e^2\lambda^2}{k^4}(-g_{\mu\alpha})(p \cdot k g^{\mu\nu} - k^{\mu}p^{\nu})(p \cdot k g^{\alpha\beta} - k^{\alpha}p^{\beta}) \\ &\quad \bar{u^{(t)}}(q_2)\gamma_{\nu}u^{(s)}(q_1)\bar{u^{(s)}}(q_1)\gamma_{\beta}u^{(t)}(q_2) \end{aligned} \tag{44}$$

Applying identities for traces of γ-matrices:

$$\begin{aligned} \frac{1}{4}|M|^2 &= \frac{4Q^2e^2\lambda^2}{k^4}(-g_{\mu\alpha})(p \cdot k g^{\mu\nu} - k^{\mu}p^{\nu})(p \cdot k g^{\alpha\beta} - k^{\alpha}p^{\beta}) \\ &\quad (4)[q_{1\nu}q_{2\beta} + q_{1\beta}q_{2\nu} - g_{\nu\beta}(q_1 \cdot q_2 - m_q^2)] \end{aligned} \tag{45}$$

Contracting over indices and eliminating any term with p^2 because $p^2 = 0$ for an external photon:

$$\frac{1}{4}|M|^2 = \frac{-32Q^2e^2\lambda^2}{k^4}[(p\cdot k)^2 m_q^2 - (p\cdot k)(k\cdot q_1)(p\cdot q_2) - (p\cdot k)(k\cdot q_2)(p\cdot q_1) + k^2(p\cdot q_1)(p\cdot q_2)] \tag{46}$$

The four-momenta in the COM frame are:

$$p = (E,\ 0,\ 0,\ E) \tag{47}$$

$$q_1 = (\sqrt{E^2 + m_q^2},\ 0,\ 0,\ -E) \tag{48}$$

$$l = (\sqrt{l_\phi^2 + m_\phi^2},\ 0,\ l_\phi \sin\theta,\ l_\phi \cos\theta) \tag{49}$$

$$q_2 = (\sqrt{l_\phi^2 + m_q^2},\ 0,\ -l_\phi \sin\theta,\ -l_\phi \cos\theta) \tag{50}$$

$$k = (\sqrt{l_\phi^2 + m_\phi^2} - E,\ 0,\ l_\phi \sin\theta,\ l_\phi \cos\theta - E) \tag{51}$$

Note that l_ϕ is not a variable, but is determined by conservation of energy.

In general, the expression for the differential cross section for two particles A and B scattering to two particles 1 and 2 is:

$$\frac{d\sigma}{d\Omega} = \frac{1}{2E_A 2E_B |v_A - v_B|} \frac{|\vec{p_1}|}{(2\pi)^2 4E_{CM}} |M(p_A, p_B \to p_1, p_2)|^2 \tag{52}$$

In this case:

$$E_A = E \tag{53}$$

$$E_B = \sqrt{E^2 + m_q^2} \tag{54}$$

$$|v_A - v_B| = \frac{\sqrt{E^2 + m_q^2} + E}{\sqrt{E^2 + m_q^2}} \tag{55}$$

$$|\vec{p_1}| = l_\phi \tag{56}$$

And:

$$E_{CM} = E + \sqrt{E^2 + m_q^2} \tag{57}$$

Substituting in these values and integrating over azimuthal angle yields:

$$\frac{d\sigma}{d\cos\theta} = \frac{l_\phi}{32\pi} \frac{|M|^2}{E(\sqrt{E^2 + m_q^2} + E)^2} \tag{58}$$

B Calculation of $e^+e^- \to \gamma\phi$ Cross Section

The Feynman diagram for $e^+e^- \to \gamma\phi$ is shown in Fig. 10. Therefore the scattering amplitude is:

$$iM = \bar{v}^{(t)}(q_2)(ie\gamma^\alpha)u^{(s)}(q_1)\frac{-ig_{\nu\alpha}}{k^2}(-4i\lambda)[p\cdot k g^{\mu\nu} - k^\mu p^\nu]\epsilon_\mu^{(r)}(p) \tag{59}$$

And the squared amplitude is:

$$\begin{aligned} |M|^2 &= \frac{16e^2\lambda^2}{k^4}\epsilon_\mu^{(r)}(p)\epsilon_a lpha^{*(r)}(p)\bar{v}^{(t)}(q_2)\gamma_\nu u^{(s)}(q_1)\bar{u}^{(s)}(q_1)\gamma_\beta v^{(t)}(q_2) \\ &\quad [p\cdot k g^{\mu\nu} - k^\mu p^\nu][p\cdot k g^{\alpha\beta} - k^\alpha p^\beta] \end{aligned} \tag{60}$$

Averaging over initial and summing over final spin and polarization states:

$$\frac{1}{4}|M|^2 = \frac{4e^2\lambda^2}{k^4}(-g_{\mu\alpha})[p\cdot k g^{\mu\nu} - k^\mu p^\nu][p\cdot k g^{\alpha\beta} - k^\alpha p^\beta]tr[(\not{q}_2 - m_e)\gamma_\nu(\not{q}_1 + m_e)\gamma_\beta] \tag{61}$$

Using the identities for traces of gamma matrices:

$$\begin{aligned} \frac{1}{4}|M|^2 &= \frac{4e^2\lambda^2}{k^4}[(p\cdot k)^2 g^\nu_\alpha g^{\alpha\beta} - p\cdot k g^\nu_\alpha k^\alpha p^\beta - p\cdot k g^{\alpha\beta}k_\alpha p^\nu + k^2 p^\nu p^\beta] \\ &\quad (4)[q_{1\beta}q_{2\nu} + q_{1\nu}q_{2\beta} - (q_1\cdot q_2 + m_e^2)g_{\nu\beta}] \end{aligned} \tag{62}$$

Multiplying out and contracting indices:

$$\begin{aligned} \frac{1}{4}|M|^2 &= \frac{32e^2\lambda^2}{k^4}[m_e^2(p\cdot k)^2 + (p\cdot k)(p\cdot q_1)(k\cdot q_2) \\ &\quad +(p\cdot k)(p\cdot q_2)(k\cdot q_1) - k^2(p\cdot q_1)(p\cdot q_2)] \end{aligned} \tag{63}$$

The four-momenta in the COM frame are:

$$q_1 = (\frac{E_{CM}}{2},\ 0,\ 0,\ q) \tag{64}$$

$$q_2 = (\frac{E_{CM}}{2},\ 0,\ 0,\ -q) \tag{65}$$

$$l = (E',\ 0,\ (E_{CM} - E')\sin\theta,\ (E_{CM} - E')\cos\theta) \tag{66}$$

$$p = (E_{CM}E',\ 0,\ -(E_{CM} - E')\sin\theta,\ -(E_{CM} - E')\cos\theta) \tag{67}$$

$$k = (E_{CM},\ 0,\ 0,\ 0) \tag{68}$$

Where:

$$E' = \frac{m_\phi^2 + E_{CM}^2}{2E_{CM}} \tag{69}$$

And:

$$q = \sqrt{\frac{E_{CM}^2}{4} - m_e^2} \tag{70}$$

Substituting these into Eq. 63:

$$\frac{1}{4}|M|^2 = \frac{32e^2\lambda^2}{E_{CM}^2}(E_{CM} - E')^2[m_e^2 + \frac{E_{CM}^2}{4} + q^2\cos\theta^2] \tag{71}$$

The general expression for the cross section of two particles A and B scattering to two particles 1 and 2 is:

$$\frac{d\sigma}{d\Omega} = \frac{1}{2E_A 2E_B|v_A - v_B|}\frac{|\vec{p_1}|}{(2\pi)^2 4E_{CM}}|M(p_A, p_B \to p_1, p_2)|^2 \tag{72}$$

In this case:

$$E_A = E_B = \frac{E_{CM}}{2} \tag{73}$$

$$|v_A - v_B| = \frac{4q}{E_{CM}} \tag{74}$$

$$|\vec{p}_1| = E_{CM} - E' \tag{75}$$

Therefore:

$$\frac{d\sigma}{d\Omega} = \frac{e^2\lambda^2}{2\pi^2}\frac{(E_{CM} - E')^3}{qE_{CM}^4}[m_e^2 + \frac{E_{CM}^2}{4} + q^2\cos\theta^2] \tag{76}$$

Substituting in $e^2 = 4\pi\alpha$ and integrating over the entire azimuthal angle:

$$\frac{d\sigma}{d\cos\theta} = 4\alpha\lambda^2\frac{(E_{CM} - E')^3}{qE_{CM}^4}[m_e^2 + \frac{E_{CM}^2}{4} + q^2\cos\theta^2] \tag{77}$$

Integrating from $\theta = 45^o$ to 135^o, or $\cos\theta = \frac{1}{\sqrt{2}}$ to $-\frac{1}{\sqrt{2}}$:

$$\sigma = 4\alpha\lambda^2\frac{(E_{CM} - E')^3}{qE_{CM}^4}[\frac{2m_e^2}{\sqrt{2}} + \frac{E_{CM}}{2\sqrt{2}} + \frac{q^2}{3\sqrt{2}} \tag{78}$$

Substituting in the expressions for E' and q:

$$\sigma = \frac{\alpha\lambda^2}{2E_{CM}^7}\frac{(E_{CM}^2 - m_\phi^2)^3}{\sqrt{\frac{E_{CM}^2}{4} - m_e^2}}[\frac{2m_e^2}{\sqrt{2}} + \frac{E_{CM}^2}{2\sqrt{2}} + \frac{1}{3\sqrt{2}}(\frac{E_{CM}^2}{4} - m_e^2)] \tag{79}$$

C Calculation of the ratio of $\Gamma(\Upsilon(1S) \to \gamma\phi)$ to $\Gamma(\Upsilon(1S) \to \mu^+\mu^-)$

The Feynman diagram for $\Upsilon(1S) \to \gamma\phi$ is shown in Fig. 13. The expression for the effective vertex in momentum space is:

$$new\ vertex = \zeta[p \cdot q g^{\mu\nu} - q^\mu p^\nu] \tag{80}$$

Therefore the scattering amplitude is:

$$iM = \epsilon_\mu^{(r)} \zeta[p \cdot q g^{\mu\nu} - q^\mu p^\nu] \frac{-ig_{\nu\alpha}}{q^2}(-4i\lambda)[q \cdot k g^{\alpha\beta} - k^\alpha q^\beta]\epsilon_\beta^{*(s)} \tag{81}$$

Contracting up $g_{\nu\alpha}$:

$$iM = \frac{-4\zeta\lambda}{q^2}\epsilon_\mu^{(r)} \zeta[p \cdot q g^{\mu\nu} - q^\mu p^\nu][q \cdot k g_\nu^\beta - k_\nu q^\beta]\epsilon_\beta^{*(s)} \tag{82}$$

Therefore the squared amplitude is:

$$|M|^2 = \frac{16\zeta^2\lambda^2}{q^4}\epsilon_\mu^{(r)}\epsilon_\delta^{*(r)}[p \cdot q g^{\mu\nu} - q^\mu p^\nu][p \cdot q g^{\delta\sigma} - q^\delta p^\sigma][q \cdot k g_\nu^\beta - k_\nu q^\beta][q \cdot k g_\sigma^\rho - k_\sigma q^\rho]\epsilon_\beta^{*(s)}\epsilon_\rho^{(s)} \tag{83}$$

Summing over initial and final spin states:

$$|M|^2 = \frac{16\zeta^2\lambda^2}{q^4}(-g_{\mu\delta})[p \cdot q g^{\mu\nu} - q^\mu p^\nu][p \cdot q g^{\delta\sigma} - q^\delta p^\sigma][q \cdot k g_\nu^\beta - k_\nu q^\beta][q \cdot k g_\sigma^\rho - k_\sigma q^\rho](-g_{\beta\rho}) \tag{84}$$

Contracting up $g_{\mu\delta}$ and $g_{\beta\rho}$:

$$|M|^2 = \frac{16\zeta^2\lambda^2}{q^4}[p \cdot q g^{\mu\nu} - q^\mu p^\nu][p \cdot q g_\mu^\sigma - q_\mu p^\sigma][q \cdot k g_\nu^\beta - k_\nu q^\beta][q \cdot k g_{\sigma\beta} - k_\sigma q_\beta] \tag{85}$$

Multiplying out and contracting indices:

$$|M|^2 = \frac{16\zeta^2\lambda^2}{q^4}[2(p \cdot q)^2 - 2q^2(p \cdot q)(p \cdot k)(q \cdot k) + p^2 q^2 (q \cdot k)^2 + q^4(p \cdot k)^2] \tag{86}$$

The four-momenta in the rest frame of the Υ are:

$$p = (m_\Upsilon,\ 0,\ 0,\ 0) \tag{87}$$

$$q = (m_\Upsilon,\ 0,\ 0,\ 0) \tag{88}$$

$$k = (E,\ 0,\ 0,\ E) \tag{89}$$

$$l = (m_\Upsilon - E,\ 0,\ 0,\ -E) \tag{90}$$

Where:

$$E = \frac{m_\Upsilon^2 - m_\phi^2}{2m_\Upsilon} \tag{91}$$

Substituting into Eq. (86):

$$|M|^2 = 8\zeta^2\lambda^2(m_\Upsilon^2 - m_\phi^2)^2 \tag{92}$$

Similarly, the Feynman diagram for $\Upsilon(1S) \to \mu^+\mu^-$ is shown in Fig. 14. Therefore the scattering amplitude is:

$$iM = \epsilon_\mu^{(r)}\zeta[p\cdot qg^{\mu\nu} - q^\mu p^\nu]\frac{-ig_{\nu\alpha}}{q^2}\bar{u}^{(s)}(l)(ie\gamma^\alpha)v^{(t)}(k) \tag{93}$$

Contracting up $g_{\nu\alpha}$:

$$iM = \frac{e\zeta}{q^2}\epsilon_\mu^{(r)}[p\cdot qg^{\mu\nu} - q^\mu p^\nu]\bar{u}^{(s)}(l)(ie\gamma_\nu)v^{(t)}(k) \tag{94}$$

Therefore the squared amplitude is:

$$|M|^2 = \frac{e^2\zeta^2}{q^4}\epsilon_\mu^{(r)}\epsilon_\delta^{*(r)}[p\cdot qg^{\mu\nu} - q^\mu p^\nu][p\cdot qg^{\delta\sigma} - q^\delta p^\sigma]\bar{u}^{(s)}(l)(ie\gamma_\nu)v^{(t)}(k)\bar{v}^{(t)}(k)(ie\gamma_\sigma)u^{(s)}(l) \tag{95}$$

Multiplying out the spinor wavefunctions:

$$|M|^2 = \frac{e^2\zeta^2}{q^4}\epsilon_\mu^{(r)}\epsilon_\delta^{*(r)}[p\cdot qg^{\mu\nu} - q^\mu p^\nu][p\cdot qg^{\delta\sigma} - q^\delta p^\sigma](\not{l} + m_\mu)\gamma_\nu(\not{k} - m_\mu)\gamma_\sigma \tag{96}$$

Using the identities for traces of gamma matrices:

$$|M|^2 = \frac{e^2\zeta^2}{q^4}\epsilon_\mu^{(r)}\epsilon_\delta^{*(r)}[p\cdot qg^{\mu\nu} - q^\mu p^\nu][p\cdot qg^{\delta\sigma} - q^\delta p^\sigma][l_\nu k_\sigma + l_\sigma k_\nu - (l\cdot k + m_\mu^2)g_{\nu\sigma}] \tag{97}$$

Summing over initial and final spin and polarization states:

$$|M|^2 = \frac{e^2\zeta^2}{q^4}(-g_{\mu\delta})[p\cdot qg^{\mu\nu} - q^\mu p^\nu][p\cdot qg^{\delta\sigma} - q^\delta p^\sigma][l_\nu k_\sigma + l_\sigma k_\nu - (l\cdot k + m_\mu^2)g_{\nu\sigma}] \tag{98}$$

$$|M|^2 = \frac{-e^2\zeta^2}{q^4}[p\cdot q g^{\mu\nu} - q^\mu p^\nu][p\cdot q g^\sigma_\mu - q_\mu p^\sigma][l_\nu k_\sigma + l_\sigma k_\nu - (l\cdot k + m_\mu^2)g_{\nu\sigma}] \quad (99)$$

Multiplying out and contracting indices:

$$|M|^2 = \frac{e^2\zeta^2}{q^4}[2(p\cdot q)(q\cdot l)(p\cdot k)+2(p\cdot q)(p\cdot l)(q\cdot k)+2m_\mu^2(p\cdot q)^2+q^2p^2(l\cdot k+m_\mu^2)-2q^2(p\cdot l)(p\cdot k)] \quad (100)$$

The four-momenta in the rest frame of the Υ are:

$$p = (m_\Upsilon,\ 0,\ 0,\ 0) \quad (101)$$

$$q = (m_\Upsilon,\ 0,\ 0,\ 0) \quad (102)$$

$$k = (\frac{m_\Upsilon}{2},\ 0,\ 0,\ k_\mu) \quad (103)$$

$$l = (\frac{m_\Upsilon}{2},\ 0,\ 0,\ -k_\mu) \quad (104)$$

Where:

$$k_\mu = \sqrt{\frac{m_\Upsilon^2}{4} - m_\mu^2} \quad (105)$$

Substituting into Eq. (100):

$$|M|^2 = e^2\zeta^2(m_\Upsilon^2 + 2m_\mu^2) \quad (106)$$

In general, the decay width for a particle A decaying to two final state particles, each with three-momentum $\vec{p}$ in the COM frame is:

$$d\Gamma = \frac{1}{m_A}\int \frac{d\Omega_{CM}}{32\pi^2}\frac{|\vec{p_1}|}{E_{CM}}|M(m_A \to p_1, p_2)|^2 \quad (107)$$

Because we are taking the ratio of the two decay widths, we only need to worry about the terms that don't cancel. In this case, because both decays have the same initial state, almost everything cancels, and all we are left with is:

$$\frac{\Gamma(\Upsilon(1S)\to\gamma\phi)}{\Gamma(\Upsilon(1S)\to\mu^+\mu^-)} = \frac{|M(\Upsilon(1S)\to\gamma\phi)|^2|\vec{p_\phi}|}{|M(\Upsilon(1S)\to\mu^+\mu^-)|^2|\vec{p_\mu}|} \quad (108)$$

Substituting from Eqs. (92) and (106):

$$\frac{\Gamma(\Upsilon(1S)\to\gamma\phi)}{\Gamma(\Upsilon(1S)\to\mu^+\mu^-)} = \frac{4\lambda^2(m_\Upsilon^2 - m_\phi^2)^3}{e^2m_\Upsilon^2(m_\Upsilon^2+2m_\mu^2)\sqrt{\frac{m_\Upsilon^2}{4}-m_\mu^2}} \quad (109)$$

D Calculation of Phi's Decay Distance

The Feynman diagram for ϕ decay is shown in Fig. 16. Therefore the scattering amplitude is:

$$iM = (-4i\lambda)[p_1 \cdot p_2 g^{\mu\nu} - p_2^\mu p_1^\nu]\epsilon_\mu^{*(r)}(p_1)\epsilon_\nu^{*(s)}(p_2) \tag{110}$$

And the squared amplitude is:

$$|M|^2 = 16\lambda^2[p_1 \cdot p_2 g^{\mu\nu} - p_2^\mu p_1^\nu][p_1 \cdot p_2 g^{\alpha\beta} - p_2^\alpha p_1^\beta]\epsilon_\mu^{*(r)}(p_1)\epsilon_\alpha^{(r)}(p_1)\epsilon_\nu^{*(s)}(p_2)\epsilon_\beta^{(s)}(p_2) \tag{111}$$

Summing over final polarization states:

$$|M|^2 = 16\lambda^2[p_1 \cdot p_2 g^{\mu\nu} - p_2^\mu p_1^\nu][p_1 \cdot p_2 g^{\alpha\beta} - p_2^\alpha p_1^\beta](-g_{\mu\alpha})(-g_{\nu\beta}) \tag{112}$$

Multiplying out and contracting indices:

$$|M|^2 = 16\lambda^2 = 32\lambda^2(p_1 \cdot p_2)^2 \tag{113}$$

The four-momenta in the COM frame are:

$$l = (m_\phi,\ 0,\ 0,\ 0) \tag{114}$$

$$p_1 = (\frac{m_\phi}{2},\ 0,\ p\sin\theta,\ p\cos\theta) \tag{115}$$

$$p_2 = (\frac{m_\phi}{2},\ 0,\ -p\sin\theta,\ -p\cos\theta) \tag{116}$$

In general, the decay width for a particle A decaying to two final state particles, each with three-momentum $\vec{p}$ in the COM frame is:

$$d\Gamma = \frac{1}{m_A}\int \frac{d\Omega_{CM}}{32\pi^2}\frac{|\vec{p_1}|}{E_{CM}}|M(m_A \to p_1, p_2)|^2 \tag{117}$$

In this case:

$$m_A = E_{CM} = m_\phi \tag{118}$$

$$\vec{p} = \frac{m_\phi}{2} \tag{119}$$

Substituting into Eq. (117):

$$\Gamma = \frac{\lambda^2 m_\phi^3}{2\pi} \tag{120}$$

Now find the mean lifetime:

$$\tau = \frac{\hbar}{\Gamma} = \frac{\hbar 2\pi}{\lambda^2 {m_\phi}^3} \tag{121}$$

Therefore the decay distance is:

$$d = \frac{c\hbar 2\pi}{\lambda^2 {m_\phi}^3} \tag{122}$$

E Calculation of the Squared Amplitude for Photon-Photon Scattering

The Feynman diagram for photon-photon scattering via the phi-photon vertex is shown in Fig. 18. Therefore the scattering amplitude is:

$$\begin{aligned} iM &= \epsilon_\mu^{(r)}(p_1)\epsilon_\nu^{(s)}(p_2)(4i\lambda)[p_1\cdot p_2 g^{\mu\nu} - p_2^\mu p_1^\nu]\frac{1}{k^2-m_\phi^2} \\ &\quad (4i\lambda)[q_1\cdot q_2 g^{\alpha\beta} - q_2^\alpha q_1^\beta]\epsilon_\alpha^{(t)}(q_1)\epsilon_\beta^{(u)}(q_2) \end{aligned} \tag{123}$$

And the squared amplitude after averaging over initial and summing over final polarization states is:

$$\begin{aligned} \frac{1}{4}|M|^2 &= \frac{1}{4}\frac{256\lambda^4}{(k^2-m_\phi^2)^2} \\ &\quad (-g_{\mu\delta})(-g_{\nu\sigma})[p_1\cdot p_2 g^{\mu\nu} - p_2^\mu p_1^\nu][p_1\cdot p_2 g^{\delta\sigma} - p_2^\delta p_1^\sigma] \\ &\quad (-g_{\alpha\rho})(-g_{\beta\omega})[q_1\cdot q_2 g^{\alpha\beta} - q_2^\alpha q_1^\beta][q_1\cdot q_2 g^{\rho\omega} - q_2^\rho q_1^\omega] \end{aligned} \tag{124}$$

Multiplying out and contracting over indices:

$$\frac{1}{4}|M|^2 = 256\lambda^4\frac{(p_1\cdot p_2)^2(q_1\cdot q_2)^2}{(k^2-m_\phi^2)^2} \tag{125}$$

Because all of the external lines are photons, the four-momenta in the COM frame are simple:

$$p_1 = (\frac{E_{CM}}{2},\ 0,\ 0,\frac{E_{CM}}{2}) \tag{126}$$

$$p_2 = (\frac{E_{CM}}{2},\ 0,\ 0,-\frac{E_{CM}}{2}) \tag{127}$$

$$q_1 = (\frac{E_{CM}}{2},\ 0,\ \frac{E_{CM}}{2}\sin\theta,\frac{E_{CM}}{2}\cos\theta) \tag{128}$$

$$q_2 = (\frac{E_{CM}}{2},\ 0,\ -\frac{E_{CM}}{2}\sin\theta,-\frac{E_{CM}}{2}\cos\theta) \tag{129}$$

$$k = (E_{CM},\ 0,\ 0,\ 0) \tag{130}$$

Substituting into Eq. (125), the final expression for the squared amplitude is:

$$\frac{1}{4}|M|^2 = \frac{16\lambda^4 E_{CM}^8}{(E_{CM}^2-m_\phi^2)^2} \tag{131}$$

F C++ Code to Calculate JLab Production Rates

```
#include <iostream.h>
#include <fstream.h>
#include <math.h>

float numInt( float, float, float, int);
float Converge( float, float, float);
float Integrand( float, float, float, float, float);

int main()
{
ifstream inFile;
ofstream outFile;

float s;
float lambda;
float m_phi;

inFile.open("tableIn.dat");
outFile.open("tableOut.dat");

//input the requisite numbers:

inFile >> s;

        while(!inFile.eof())
{
inFile >> lambda;

inFile >> m_phi;

outFile << "For s= " << s << ", lambda= " << lambda
   << ", and m_phi= " << m_phi
   << " the number of events per year is ";

outFile << Converge(s, lambda, m_phi) << "." << endl;

           inFile >> s;
        }

outFile.close();

return 0;
}

//*********************************************************
```

```
//numerical integration function:

float numInt( float s, float lambda, float m_phi, int numSteps )
{
const float M_PROTON = .938;
      const float CONVERSION = .389379E9;
const float LUMINOSITY = 36.0*24.0*365.25;

      float x; //variables of integration
      float ct;

      float x_stepSize;                   //size of the rectangles
float ct_stepSize;

float total; //to use in integration
//loops

float x1; //roots from energy
float x2; //constraint

float lower_x; //lower limit of x
//integration

//find the lower limit of x integration:

x1 = (-(2 * m_phi * M_PROTON - s) + sqrt(pow((2 *
     m_phi * M_PROTON - s),2) - 4 * pow (M_PROTON, 2) *
     pow(m_phi, 2))) / (2 * pow(M_PROTON ,2));

x2 = (-(2 * m_phi * M_PROTON - s) - sqrt(pow((2 *
     m_phi * M_PROTON - s),2) - 4 * pow (M_PROTON, 2) *
       pow(m_phi, 2))) / (2 * pow(M_PROTON ,2));

if ( x1 <= 1 )
lower_x = x1;

else lower_x = x2;

//do the integration:

x_stepSize = (1.0 - lower_x ) / numSteps;

ct_stepSize = 2.0 / numSteps;

total = 0.0;
```

```
for (int j = 1; j <= numSteps; j++)
{
ct = (-2.0 + (2.0*j-1.0)*ct_stepSize)/2.0;

for (int i = 1; i <= numSteps; i++)
{
x = (2.0*lower_x +(2.0*i-1.0) *
                                              x_stepSize)/2.0;

total = total +
Integrand(s, lambda,
m_phi, x, ct)*
CONVERSION*LUMINOSITY*
         ct_stepSize * x_stepSize;
}

}

      return total;
}

//*********************************************************

//this function makes numInt converge, and is a modified version of
//one found in Numerical Recipes for C:

float Converge( float s, float lambda, float m_phi )
{
const float EPS=.01;
const float J_MAX=1E9;

float ans;
float old_ans = -1E30;
int j = 150;

do { ans = numInt(s, lambda, m_phi, j);

cout << j << ans  << endl;

if (fabs(ans-old_ans) < EPS * fabs(old_ans)) return ans;
if (ans==0.0 && old_ans==0.0) return ans;

old_ans = ans;
j = j*3;

} while( j <= J_MAX );
```

```
return 0;
}

//*********************************************************

//this is the integrand:

float Integrand( float s, float lambda, float m_phi, float x,
  float ct )
{
const float M_PROTON = .938;
const float PI = 3.14159;
const float e = sqrt(4*PI/137);

float s_hat, m_q, E, l_phi;
float pdotk, pdotq1, pdotq2, kdotq1, kdotq2, ksquared;
float upMsquared, downMsquared;
float du, dd;
float u_sea, d_sea, s_sea, u_v, d_v;
float integrand;

s_hat = x*s;

m_q = x*M_PROTON;

E = (s_hat - pow(m_q,2))/2/sqrt(s_hat);

l_phi = sqrt(s_hat/4 - pow(m_phi,2)/2 - pow(m_q,2)/2 +
pow(m_phi,4)/4/s_hat + pow(m_q,4)/4/s_hat -
pow(m_phi,2)*pow(m_q,2)/2/s_hat);

pdotk = E*(sqrt(pow(l_phi,2)+pow(m_phi,2))-l_phi*ct);

pdotq1 = E*(sqrt(pow(E,2)+pow(m_q,2))+pow(E,2));

pdotq2 = E*(sqrt(pow(l_phi,2)+pow(m_q,2))+l_phi*ct);

kdotq1 = sqrt(pow(E,2)+pow(m_q,2))
 *(sqrt(pow(l_phi,2)+pow(m_phi,2))-E)
 + E*(l_phi*ct-E);

kdotq2 = 2*pow(l_phi,2) + pow(m_phi,2)
 - E*(sqrt(pow(l_phi,2)+pow(m_phi,2))+l_phi*ct);

ksquared = pow(m_phi,2)
   + 2*E*(l_phi*ct - sqrt(pow(l_phi,2)+pow(m_phi,2)));
```

```
upMsquared = -32.0*(4.0/9.0)*pow(e,2)*pow(lambda,2)
     *(pow(pdotk,2)*pow(m_q,2) - pdotk*kdotq1*pdotq2
     - pdotk*pdotq1*kdotq2 + ksquared*pdotq1*pdotq2)
     /pow(ksquared,2);

downMsquared = -32.0*(1.0/9.0)*pow(e,2)*pow(lambda,2)
       *(pow(pdotk,2)*pow(m_q,2) - pdotk*kdotq1*pdotq2
       - pdotk*pdotq1*kdotq2 + ksquared*pdotq1*pdotq2)
       /pow(ksquared,2);

du = upMsquared*l_phi/64/PI/E
     /sqrt(pow(E,2)+pow(m_q,2))/sqrt(s_hat);

dd = downMsquared*l_phi/64/PI/E
     /sqrt(pow(E,2)+pow(m_q,2))/sqrt(s_hat);

u_sea = .186*pow((1-x),7)/x;

d_sea = u_sea;

s_sea = .5*u_sea;

u_v = 2*1.094*pow((1-x),3)/sqrt(x);

d_v = 1.125*1.094*pow((1-x),4)/sqrt(x);

integrand = (du*(u_v + 2*u_sea) + dd*(d_v + 2*d_sea + 2*s_sea));

return integrand;
}
```

References

[1] R. Holdom, Phys. Lett. **166B**, 196 (1986).

[2] S. Davidson, B. Campbell, and D. Bailey, Phys. Rev. D **43**, 2314 (1991).

[3] M. I. Dobroliubov and A. Yu. Ignatiev, Phys. Rev. Lett. **65**, 679 (1990).

[4] H. Goldberg and L. J. Hall, Phys. Lett. B **174**, 151 (1986).

[5] Michael E. Peskin and Daniel V. Schroeder, *An Introduction to Quantum Field Theory*, (Addison-Wesley, Reading, MA, 1995).

[6] Carl E. Carlson, *private communication.*

[7] L3 Collaboration, O. Adriani *et al.*, Phys. Lett. B **292**, 463-471 (1992).

[8] CLEO Collaboration, R. Balest *et al.*, Phys. Rev. D **51**, 2053-2060 (1995).

[9] F. Wilczek, Phys. Rev. Lett. **39**, 1304-1306 (1977).

[10] Particle Data Group, C. Caso *et al.*, Eur. Phys. J. **C3**, 1 (1998).

[11] D.L. Burke *et al.*, Phys. Rev. Lett. **79**, 1626-1629 (1997).

[12] Donald H. Perkins, *Introduction to High Energy Physics*, (Addison-Wesley, Menlo Park, CA, 1987).

[13] Hall D Design Report — Version 2.0, *http://dustbunny.physics.indiana.edu/~ dzierba/newhd/.*